VERTEX SPECTROMETER: SOLENOID VERSUS DIPOLE MAGNET A COMPARATIVE STUDY

Klaus P. Pretzl
Max Planck Institute for Physics and Astrophysics

Introduction

The function of a vertex spectrometer is to measure the properties of low-energy particles which are produced at large angles to the forward direction. The best known and commonly used vertex spectrometer is a bubble chamber. Recently large spectrometers have been built which use vertex detectors (in a solenoid or a dipole field) equipped with spark chambers, wire chambers, proportional wire chambers, and streamer chambers. The variety of presently used spectrometers and vertex detectors shows that it is almost impossible to construct a universal instrument.[1]

Many papers have been written which study many aspects of spectrometers and vertex detectors.[2-10] In designing a multipurpose multiparticle spectrometer facility for doing physics at NAL and CERN II accelerators, we are faced with many of these previously studied problems, in particular the question whether a dipole or a solenoidal field would be the better choice for a vertex spectrometer.

It is the purpose of this study to discuss and to compare some of the properties offered by a vertex detector using a dipole field or a solenoidal field.

To be able to make any quantitative statements we have to work with a model. The model has been chosen to be very simple and does not represent the best solution for a vertex spectrometer. The expressions we derive for the momentum resolution and the acceptance (p_T versus p_L) are only approximations. Multiple scattering is not taken into account here. In any case it affects the results for both vertex spectrometers in the same way.

A. Momentum Resolution

1. Solenoid

We assume that the incident beam travels along the axis of the solenoid (the z axis). We further assume that the target is located on the z axis and inside the solenoidal field. In our model-spectrometer, which is schematically sketched in Fig. 1(a), we have the target surrounded by a streamer chamber. The streamer chamber can be replaced by planar and (or) cylindrical proportional wire chambers, if high beam intensities are required. Downstream of the streamer chamber and the target we place wire-chamber planes perpendicular to the z axis. To follow the particle trajectory outside the magnetic field we have a wire chamber telescope downstream of the solenoid.

The trajectory of a particle which emerges from the target at a production angle θ and travels in the axial field of the solenoid describes a helix. It can be expressed in polar coordinates

$$r = D \cdot \sin \phi$$
$$z = D \cdot \phi \cdot \cot \theta, \tag{1}$$

r is the radius vector, D = 2R is the diameter of the helix and ϕ the angle of rotation. The axial field of the solenoid rotates the transverse momentum vector p_T of the particle. The rotation ϕ of the p_T vector can directly be measured by the streamer chamber and the wire-chamber planes inside the vertex detector. The intercepts of the particle trajectory with the chambers describe a circle in the x,y plane with the radius

$$R = \frac{33.36\, p_T}{B}\ [m]. \tag{2}$$

We measure p_T in GeV/c and B in kG. For illustration see Fig. 2. By measuring R we can directly determine the transverse momentum p_T of the particle.

If the particle has a transverse momentum p_T we can describe its longitudinal momentum p_L by measuring the angle of rotation ϕ. We obtain

$$2\phi = \frac{B \cdot z}{33.36\, p_L}\ [rad], \tag{3}$$

where z is the length of the solenoidal field. Obviously particles with $p_T = 0$ traveling along the field lines of the solenoid cannot be momentum analyzed. Figure 3 illustrates the angle of rotation 2ϕ versus p_L in a solenoid with a length z = 3.0 m and field B = 20 kG.

The diameter D_{max} of a solenoid, the maximum displacement 2R of a particle trajectory from the central beam line and p_T are related by

$$D_{max} = 4R = \frac{4 p_T \cdot 33.36}{B}\ [m].$$

Figure 4 shows the variation of D_{max} with p_T for various field strengths (B = 10, 20, 25, 50 kG). For a given B = 20 kG and $D_{max} = 2$m all particles with $p_L \neq 0$ and $p_T \leq 0.3$ GeV/c will exit the ends of the solenoid. Their trajectories can then be followed by the downstream telescope.

With the definitions

$$S = \frac{r^2}{8R} \text{ and } \tan\theta = \frac{p_T}{p_L},$$

we can easily derive from Eqs. (1) a relation between p_T and the sagitta S .

$$p_T = \frac{8 \cdot 33.36}{B}\left(\frac{p_L}{z}\right)^2 \cdot S.$$

Assuming the measurement error in B and z is small compared to that of S we obtain for the error in p_T

$$\Delta p_T = \frac{8 \cdot 33.36}{B}\left(\frac{p_L}{z}\right)^2 \cdot \Delta S. \tag{4}$$

The relation between p_T and p_L is given via

$$\frac{p_L}{p_T} = \frac{z}{r}.$$

We assume $\Delta z/z$ is small and obtain

$$\frac{\Delta p_T}{p_T} = \frac{\Delta p_L}{p_L}. \tag{5}$$

The total momentum resolution in a solenoid is given by using the expressions in (4) and (5)

$$\frac{\Delta p}{p} = \frac{8 \cdot 33.36}{B \cdot p_T} \left(\frac{p_L}{z}\right)^2 \Delta S , \tag{6}$$

with $p = (p_T^2 + p_L^2)^{\frac{1}{2}}$. For a given B and ΔS the momentum resolution in a solenoid spectrometer goes as $(p_L/z)^2$. Because of the axial symmetry of the field the momentum resolution does not depend on the azimuthal angle. Hence the azimuthal angle bias for measuring the decay of N^* resonances is greatly reduced in a solenoidal compared to a dipole field. However, when studying correlations with the forward-going boson system (e.g., $\pi N \to \rho N^*$) the azimuthal symmetry also depends strongly on the horizontal and vertical acceptance of the downstream spectrometer magnets.

2. Dipole

Figure 5 schematically illustrates an analogous spectrometer model with a dipole field at the vertex. The momentum resolution in a dipole vertex spectrometer is given by

$$\frac{\Delta p}{p} = \frac{8 \cdot 33.36}{B} \frac{p}{z^2} \Delta S , \tag{7}$$

z is the distance from the target to the downstream end of the magnet. For particles with $p_T << p_L$ the above formula can be rewritten

$$\frac{\Delta p}{p} = \frac{8 \cdot 33.36 \cdot p_L}{B \cdot z^2} \Delta S. \tag{8}$$

We note that $\Delta p/p$ increases only like p_L/z^2 as compared to $(p_L/z)^2$ in the solenoid. For $p_T = p_L$ the momentum resolution in the solenoid and dipole spectrometer is equally good.

In Fig. 6, the momentum resolutions of a dipole and a solenoid are shown as a function of p_L. We assume for both cases a field B = 20 kG, ΔS = 0.25 mm, z = 3.0 m, and a fixed p_T = 0.3 GeV/c.

In hadronic reactions particles have an average p_T which is smaller than 0.6 GeV/c and independent of the incident beam energy. Hence, for reactions which include particles with $p_L > 0.6$ GeV/c, the dipole vertex spectrometer yields a better momentum resolution.

We consider now the case where the production plane of the particles is parallel to the dipole field ($\phi' = 0$). For particles with $p_L >> p_T$ formula (8) is still valid. However, for particles with $p_T \geq p_L$, which travel almost parallel to the dipole field, we have to modify formula (8). For $p_T > p_L$ we obtain the approximate expression for the momentum resolution

$$\frac{\Delta p}{p} \sim \frac{8 \cdot 33.36 \cdot p_T \cdot 4}{B \cdot \cos\theta \, g^2} \Delta S , \tag{9}$$

with $\cos\theta = p_L/p$ and g = gap of dipole magnet.

3. Increase in Momentum Resolution by Combined Particle Track Measurement Inside and Outside the Magnetic Field of a Dipole or a Solenoid Vertex Detector

We restrict ourselves to the simplest arrangement as shown in Figs. 1(a) and 5(a) for a solenoid and a dipole vertex spectrometer. Extending our measurements outside the field we obtain for the bend angle α of a particle after traversing a dipole field

$$\frac{\alpha}{2} = \frac{x_1 - x_2}{z} - \frac{x_2 - x_3}{L}.$$

The variables are explained in Fig. 5(b). If we assume an equal spatial resolution in all detectors like $\Delta x_1 = \Delta x_2 = \Delta x_3 = \Delta x$, we obtain for the error in the angle measurement

$$\frac{\Delta\alpha}{2} = \Delta x \sqrt{\left(\frac{1}{z} + \frac{1}{L}\right)^2 + \frac{1}{z^2} + \frac{1}{L^2}}$$

with L = lever arm of wire-chamber telescope after the magnet and z = distance between target and downstream end of the magnet. For L = z we obtain

$$\Delta\alpha = \frac{4 \cdot g \ \Delta x}{z}, \tag{10}$$

and for L >> z

$$\Delta\alpha = \frac{2.8 \ \Delta x}{z}. \tag{11}$$

This has to be compared with $\Delta\alpha = (8 \cdot \Delta x/z)(1.5)^{\frac{1}{2}}$ which will be reached with a sagitta measurement inside the magnet only. By neglecting multiple scattering and fringe field effects the momentum resolution in a dipole vertex-spectrometer can be improved by approximately a factor 3.5 if the particle trajectory is followed outside the magnet.

A particle leaving the solenoid off axis has to travel through the fringe field of the solenoid. The radial component of the fringe field compensates the forces on the particle in such a way that the radius vector always projects back to the axis from where the particle originated.[11] This is illustrated in Fig. 1(b). The difference Δz between the origin of the particle and the intercept of the radius vector with the z axis depends on the longitudinal momentum of the particle. For particles with relatively large p_L (and small rotational angles 2ϕ) this distance is not very well measurable and therefore would not contribute to increase the analysis power of the solenoid.

Since it does not seem practical to track particles through the solenoid fringe field, it is better to measure their production angle and momentum, if possible, inside the good field region of the solenoid and, if not possible, in a downstream spectrometer.

B. Acceptance

In calculating the acceptance as a function of the basic dipole and solenoid parameters (field, field volume, and detector geometry) we again restrict ourselves to a very simple model by making some approximations. For a given momentum resolution $\Delta p = 0.14\,\text{GeV/c}$ we will calculate the p_T versus p_L acceptance boundaries for the solenoid and dipole vertex spectrometer geometries of Figs. 1(a) and 5(a) respectively.

1. Solenoid Acceptance Boundaries

The p_T versus p_L acceptance boundary can be derived from Eq. (1)

$$r = \frac{2 \cdot 33.36 \, p_T}{B} \sin\left(\frac{B \cdot z}{2 \cdot 33.36 \, p_L}\right). \tag{15}$$

With the above formula we can calculate the acceptance boundary for particles which travel through the solenoid and intercept the wire chambers at positions z downstream of the target. Figure 7 illustrates a p_T versus p_L acceptance boundary for a solenoid diameter D = 2 m, a target to wire chamber distance z = 3 m and several field strengths of B = 10, 20, 25, 50 kG. It

can be seen that all particles with $p_L > 0$ and p_T below the plateau value, as shown in Fig. 7, will intercept the wire chamber at the downstream end of the solenoid.

To obtain the p_T versus p_L acceptance for a given momentum resolution Δp we have to make certain approximations for the two cases $p_L \geq p_T$ and $p_T \geq p_L$:

a) For $p_L \geq p_T$ formula (15) can be approximated by

$$p_T \leq \frac{r}{z} p_L = \frac{2R}{z} p_L$$

and formula (6) by

$$p_T \geq \frac{8 \cdot 33.36\, p_L^3}{B \cdot \Delta p \cdot z^2} \Delta S.$$

b) For $p_T \geq p_L$ we obtain from expression (6) the following approximate boundary condition for p_T

$$p_T^2 \leq \frac{\Delta p B \cdot r^2}{8 \cdot 33.36 \cdot \Delta S}$$

which is independent of p_L.

The shaded portion in Fig. 8 represents the p_T versus p_L acceptance for a solenoid with D = 2 m, length z = 3 m, and a field B = 20 kG as calculated from the above boundary conditions. The momentum resolution Δp was assumed to be a pion mass and ΔS = 0.25 mm.

The rabbit ears in Fig. 8 are due to the particular choice of wire-chamber geometry in the solenoid. The deep cutouts are due to particles which get lost in the drift space between the wire chambers. By adding more chambers the envelope in Fig. 8 can be smoothed out. However, it should be kept in mind that multiple scattering introduced by additional chambers may reduce considerably the p_T versus p_L acceptance region for good momentum resolution.

Particles with small p_T, independent of their p_L, will not be measured well by the solenoid. This has to be taken into account when designing a downstream spectrometer. At high energies the charged particle multiplicity of fast forward-going particles is very high, as recent NAL bubble-chamber exposures show. It will be very difficult to resolve individual particle tracks within such a fast forward-going jet with a detector system of wire chambers and streamer chambers. However, the production angle of these particles may be measured via small area, high resolution chambers (drift chambers with 100μ resolution) placed along the axis of the solenoid.

In our calculations we have not considered the acceptance of backward scattered particles (particles with negative p_L). By pushing the target far enough inside the magnetic field and by providing wire chambers upstream of the target, particles with negative p_L can well be accepted and momentum analyzed by the vertex spectrometer. The acceptance calculations are analogous to those previously shown.

2. Dipole Acceptance Boundaries

In order to make a fair comparison we choose a model dipole vertex detector [Fig. 5(a)] with approximately the same magnetic field volume as the solenoid. The dipole magnet has a width of W = 2 m, a gap of g = 1.5 m, a length of z = 3.0 m (which is the distance from the target to the downstream end of the magnet) and a field of 20 kG. Figure 9 explains the parameters which we use to derive the approximate acceptance boundaries. We write

$$\sin\left(\frac{\alpha}{2}+\theta\right) = \frac{W}{4R\sin\frac{\alpha}{2}}$$

$$\sin\frac{\alpha}{2} = \frac{z}{2R\cos\left(\frac{\alpha}{2}+\theta\right)}$$

with $\alpha = B \cdot z/33.36 \cdot p$ being the bend angle and $\theta = p_T/p_L$ the production angle. We then obtain

$$\frac{W}{z} = 2\tan\left(\frac{B \cdot z}{2 \cdot 33.36\,p}+\frac{p_T}{p_L}\right). \tag{16}$$

First we consider the case where the production plane of the particles is perpendicular ($\phi' = 90°$) to the dipole field. Using the expressions in (7) and (15) we derive the approximate acceptance boundaries for $p_L \geq p_T$ and $p_T \geq p_L$:

a) For $p_L \geq p_T$

$$p_L \geq (0.03\ Bz + 2p_T)\frac{z}{W}$$

$$p_L^2 \geq \frac{\Delta p \cdot B \cdot z^2}{8 \cdot 33.36 \cdot \Delta S}.$$

b) For $p_T \geq p_L$

$$p_T^2 \leq \frac{\Delta p \cdot B \cdot W^2}{8 \cdot 4 \cdot 33.36\,\Delta S}.$$

Particles which are produced in a plane parallel to the dipole field ($\phi' = 0°$) have the following acceptance boundaries. For $p_L \geq p_T$

$$p_L \geq (0.03Bz + 2p_T)\frac{z}{g}$$

$$p_L^2 \leq \frac{\Delta p \cdot B \cdot z^2}{8 \cdot 33.36\,\Delta S}$$

for $p_T \geq p_L$ we obtain from expression (9) with $\cos\theta = p_L/p_T$

$$p_T^3 \leq \frac{\Delta p \cdot B \cdot g^2 p_L}{8 \cdot 33.36 \cdot 4 \cdot \Delta S}.$$

The shaded area in Figs. 10 and 11 represents the acceptance boundaries for particles with a production plane ($\phi' = 90°$) perpendicular and parallel ($\phi' = 0°$) to the dipole field. The momentum resolution was assumed to be one pion mass and $\Delta S = 0.25$ mm as before. The curve in Fig. 12 shows the enlargement of the p_T versus p_L acceptance due to particle track measurement outside the magnetic field (for $L = 2z$).

It can be concluded that particles with small p_L which are produced in a plane parallel to the dipole field will not be momentum-analyzed well in a dipole vertex spectrometer. There will exist an azimuthal angle bias when studying decay angles of N^* resonance states. However, as long as the trigger system does not exclude rotational symmetry of events around the incident beam axis and the magnet gap is adequately large, one can usually correct this effect as has been shown by many bubble-chamber experiments in the past.

To assure rotational symmetry when studying correlations with the fast forward-going boson system the downstream spectrometer magnets should have a large horizontal and vertical acceptance.

We did not calculate the acceptance for backward scattered particles. However, it can be easily derived from the above formulae.

Compared to the solenoid we obtain a larger p_T versus p_L acceptance with a dipole vertex detector.

C. Summary and Conclusions

In this section we will summarize some of the properties which are offered by a solenoid and a dipole vertex spectrometer. We should keep in mind that all comparisons we make are based on the assumption that both vertex spectrometers have approximately the same field volume and the same detector arrangement.

1. Momentum Measurement and Momentum Resolution

The transverse and the longitudinal momentum measurement seem to be nicely decoupled in a solenoid. As was described in Section A.1. and Fig. 2, p_T can directly be extracted by measuring the projected radius R of the helix and p_L by measuring the rotation angle ϕ of the p_T vector. Good momentum resolution can be obtained for particles with large p_T and small p_L. Particles with small p_T are poorly analyzed by the solenoid.

The dipole seems to yield better momentum resolution for particles with $p_L/p_T \geq 1$ (Fig. 6). Since in hadronic reactions the average transverse momentum is smaller than 0.6 GeV/c, one buys better resolution with a dipole magnet than with a solenoid. For $p_L \approx p_T$ the solenoid and the dipole field give comparable resolutions. Particles with $p_L < p_T$ which are produced in a plane parallel to the dipole field are not momentum analyzed well by the dipole.

2. Acceptance

The acceptance contours in Figs. 8 and 10-12 show that in general the dipole vertex spectrometer has a larger p_T versus p_L acceptance compared to the solenoid. Particles with a p_L of up to 20 GeV/c and a p_T of up to 4.5 GeV/c are measured well with a dipole magnet. If one would restrict the physics interest only up to 20 GeV/c incident energy a dipole vertex spectrometer replaces a downstream spectrometer as in the case of the OMEGA project at CERN.

The solenoid, however, when applied to physics in external beams, always needs a downstream spectrometer if one wishes to analyze particles with small p_T and large p_L. This statement does not apply to physics at intersecting storage rings, where the solenoidal field offers many advantages over a dipole field.[12-14]

At NAL and CERN II energies, however, both the dipole and the solenoid vertex spectrometer will have to be backed up by a downstream spectrometer.

The solenoid field, because of its rotational symmetry around the incident beam axis, helps to minimize an azimuthal angle bias. In a dipole vertex detector this bias can be corrected, provided:

1. The selective trigger does not disturb the cylindrical symmetry of events and the magnet aperture is adequately large.

2. The downstream spectrometer has a large enough aperture to analyze all forward-going particles, independent of the rotation of their production plane.

In any case, particles which emerge from the target around 90° have a momentum not larger than a proton mass and their momentum analysis to about one pion mass does not require high resolution. The solid angle within which they will not be momentum analyzed well in a dipole field is a few millisteradian (for $p_T \leq 1.0$ GeV/c).

3. Matching to a Downstream Spectrometer

The vertex spectrometer being part of a modular system has to be matched to a downstream spectrometer. A certain drift space between the vertex magnet and the first magnet of the downstream spectrometer is needed for particle identification.

To optimize this drift space a dipole vertex magnet offers more flexibility, since its p_T versus p_L acceptance with good momentum resolution is larger. The dipole magnet is capable of analyzing particles with an accuracy of one pion mass up to momenta of about 20 GeV/c, while the corresponding limit for good resolution in the solenoid is 5 GeV/c for $p_T = 0.3$ GeV/c (Figs. 8 and 10). The drift space can be used to increase the analysis power of the dipole magnet (Section A. 3 and Fig. 12).

Ray tracing through a region where the fringe field of the solenoid meets the fringe field of the dipole magnet may be computer time consuming. In practice one would perhaps try to avoid that by independently tracing the particles through the good field region of the solenoid and the downstream spectrometer. The two tracks, when meeting within a couple of millimeters in the fringe field region between the vertex and the downstream magnet, will then be identified as being one and the same track.

When using dipole magnets with very good field uniformity (for example picture frame magnets) for the vertex and downstream spectrometer, ray tracing is possible with reasonable computer time consumption.

4. Particle Identification

Particle identification by time of flight inside the vertex detector is difficult since the available drift lengths are very short. Figure 13 illustrates the possibility to identify particles for a given time of flight resolution $\Delta\tau = 0.3$ nsec fwhm as a function of drift length d (meter) and momentum p (GeV/c).

All charged particles with $p_T \leq 0.3$ GeV/c (for B = 20 kG and $p_T \leq 0.75$ GeV/c for B = 50 kG) and $p_L \neq 0$ exit the ends of the solenoid and can be identified by either time of flight or Cerenkov counters (Figs. 4 and 7). If aluminum embedded superconductors would be available[14] (with ≤ 1 rad length) it would be possible to put time-of-flight counters in a space between the solenoid coil and the iron return yoke.

A dipole magnet, with removable return iron, like the OMEGA magnet, would allow particle identification outside the vertex detector within certain solid angle limitations.

When using a streamer chamber it is possible to separate pions from protons up to approximately 1 GeV/c by ionization measurements.[15]

5. Optical Vertex Detector

We restrict our considerations to the use of a streamer chamber in a vertex spectrometer. With a memory time of one microsecond the streamer chamber can, depending on the beam structure, tolerate rates of a few times 10^6 particles per second.[15] The electrical field of the

chamber, the magnetic field of the dipole or solenoid and the axis of view have to be parallel to obtain good resolution. If mounted in a solenoid the chamber planes are perpendicular to the incident beam axis and can be viewed by an optical system with a plumbicon or vidicon read out from the upstream axis of the solenoid [Fig. 1(a)]. A chamber of one meter length would have 10×10 cm gaps. Any jet of fast forward going particles would have to go through all the gaps of the chamber and likely produces flairs, which fuzz out the picture quality. In order to prevent this, the chamber has to be operated in an avalanche mode, where the light output of the streamers is less than if operated in the streamer mode. Image intensifiers will most likely be necessary in this case.

If mounted in a dipole vertex detector the streamer chamber planes would be parallel to the dipole field and be viewed through a hole, which could be obtained by removing one of the pole pieces. Because of the optical access the solid angle for trigger and (or) time-of-flight counters will be limited. In this position the chamber can be operated in the streamer mode. For reasons of better resolution however the avalanche mode may also be preferred in this case.

6. Pattern Recognition

As has been pointed out by G. Luste[3] the solenoid offers nice pattern recognition features, which help to reduce valuable computer time for event reconstruction inside the vertex detector. With evenly spaced chambers along the solenoid axis a simple procedure of searching for equal chord lengths in the xy plane of the solenoid gives good results with minimum computer time.

This algorithm has only very limited application to a dipole vertex spectrometer. Other pattern recognition methods[16-18] have been studied for dipole vertex spectrometers.

The fast forward going jet of particles will be dispersed by the dipole magnet, which in some cases helps to reduce the pattern recognition problem. The solenoid does not disperse these particles. However, for experiments which require very high intense incident beams (for example electron or photon beams), this can be an advantage, because the solenoidal field prevents spreading the incident beam and the associated junk over the vertex detector.

7. Access

In order to use a large spectrometer facility most efficiently the down time due to maintenance or to changes in the particle detection system has to be kept a minimum. Hence a vertex detector which contains detectors of complicated nature has to be easily accessible. The OMEGA magnet, which has removable modular iron return yokes and pole pieces allowing access to the detector system from all sides seem to have solved this problem satisfactorily. The increase in the total magnet cost due to the removable iron return yokes was approximately $\leq 10\%$.[19] A modular return yoke offers also the possibility to set up detectors around the dipole magnet, for example, slow proton, neutron or π^0 triggers or time-of-flight counters.

If it is possible to build stabilized superconductors out of a material which does not absorb high-energy particles, counters can be put around the solenoid to detect or trigger on particles produced at large angles.

8. Cost

Since the cost for the particle detection system in a dipole and a solenoid vertex spectrometer is very similar, we are quoting a cost estimate only for the magnets.

Several approximative cost estimates[20] have been made for a 3-m long solenoid with an inner diameter of 2 m and a field of 20-25 kG. The average of these estimates is $1.0±0.4 millions. This amount includes the cost of the superconducting coils, the cryostat, the vacuum system, the power supply, the controls and the return iron.

This can be compared with the corresponding costs of over $2.0 millions for the superconducting CERN OMEGA magnet.[21] The general characteristics of this dipole magnet are maximum field = 20 kG, inner diameter of circular coils = 3.0 m, free gap between coils = 1.5 m and free gap between poles = 2.0 m.

A large fraction of the cost difference is explained by the different amount of iron used for the solenoid (average 150 tons) as compared to the OMEGA-dipole magnet (1300 tons).

9. Conclusion

We believe that a solenoid vertex spectrometer offers many very attractive features and is a versatile instrument for physics at NAL and CERN II accelerators. However, if we put the emphasis on accessibility and on the possibility of setting up detectors around the vertex magnet, we believe that a large dipole magnet with removable return yokes and pole pieces offers more flexibility than a solenoid. We think these features are worth the increase in cost.

It should be kept in mind, when designing a large multiparticle spectrometer facility for NAL or CERN II, that in contrast to the downstream spectrometer the vertex detector will not scale with the incident beam energy. By adding more $\int Bdl$ at a later time a downstream spectrometer can be updated for use at higher energies. The vertex spectrometer however, which is densely packed with complicated particle detection systems, should be dimensioned from the beginning generously enough to avoid a duplication in effort and cost at a later time. In essence we propose a vertex dipole magnet of approximately the size of the OMEGA.

Acknowledgments

I would like to thank all my colleagues of the Summer Study, in particular G. Ascoli, W. Baker, G. Buschhorn, R. Diebold, R. Edelstein, G. Luste, A. Michelini, and P. Schacht for helpful discussions and valuable comments.

References

[1] A. Michelini, Spectrometers for High Energy Physics, Invited talk presented at the International Conference on Instrumentation for High Energy Physics, Frascati, May 8-12, 1973.

[2] W. K. H. Panofsky, Proceedings of the International Conference on Instrumentation for High Energy Physics, Dubna, 1, 73 (1970).

[3] G. J. Luste, The Solenoid Vertex Spectrometer - a Simulation Study, SLAC-152, June 1972; also Comments on the Solenoid Vertex Spectrometer, Frascati Conference, 1973.

[4] D. I. Meyer, Vertex Detectors Employing Magnetic Fields Along the Beam Axis, NAL 1970 Summer Study Report, p. 161-163.

[5] L. S. Osborne, Design Criteria for a Magnetic Spectrometer, NAL 1969 Summer Study Report 3, p. 267.

[6] W. Baker et al., Design Criteria for Spectrometers, NAL Report (1970).

[7] B. D. Hyams et al., A Multiparticle Forward Spectrometer, ECFA Report, Tirrenia, 1, 342 (1972).

[8] W. Koch, A Multiparticle Forward Spectrometer, contribution to the ECFA study week on 300-GeV Accelerator, Tirrenia, 1971.

[9] B. R. French and L. Mandelli, OMEGA Versus 100 GeV, CERN/D. Ph. II/Phys 72-8 (1972).

[10] Ascoli, Osborne, and Selove, The Alpha Project, NAL 1969 Summer Study Report, p. 279.

[11] W. Panofsky and M. Phillips, Classical Electricity and Magnetism, 2 ed., Addison-Wesley 1962.

[12] L. Criegee et al., Pluto 4π Detector for Doris, International Conference on Instrumentation for High Energy Physics, Frascati, May 8-12, 1973.

[13] R. F. Schwitters, The SPEAR Magnetic Detector, Proceedings of the XVI International Conference on High Energy Physics 2, 433 (1972).

[14] M. L. Stevenson, Conceptual Design of a Hybrid Detector for Electron Physics at ISABELLE and PEP, ISABELLE Summer Study Report, p. 182 (1972).

[15] V. Eckardt et al., Electroproduction in a Streamer Chamber at 7.2 GeV and $0.3 < Q^2 < 1.5$ GeV^2, Part I and II, paper 639 and 640 submitted to the XVI International Conference on High Energy Physics, Chicago-Batavia, 1972, and V. Eckardt, private communication.

[16] J. C. Lassalle, OM-development notes, DD division program ROMEO.

[17] Frank Turkot, private communication.

[18] M. Hansroul et al., Hardware Processors for Pattern Recognition Tasks in Wire Chamber Data, International Conference on Instrumentation for High Energy Physics, Frascati, May 8-12, 1973.

[19] A. Michelini, private communication.

[20] A. Manz and R. Settles, Internal Report, Max Planck Institute for Physics and Astrophysics Munich, Detoeuf, Levegue (Saclay) private communication; IN2P3-Munich-Saclay collaboration, SPS North Area Spectrometer Study; D. Leith (SLAC) private communication; R. Fast (NAL) private communication.

[21] The OMEGA Project, NP Division Internal Report 68-11, p. 67.

SOLENOID VERTEX SPECTROMETER

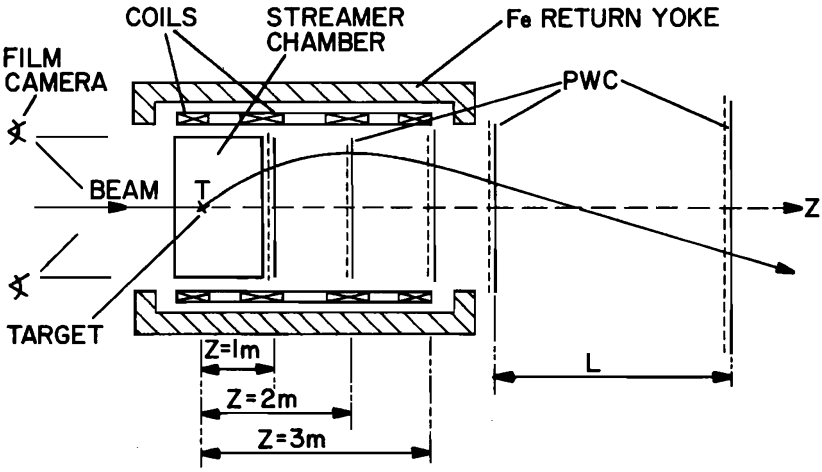

FIG. 1a

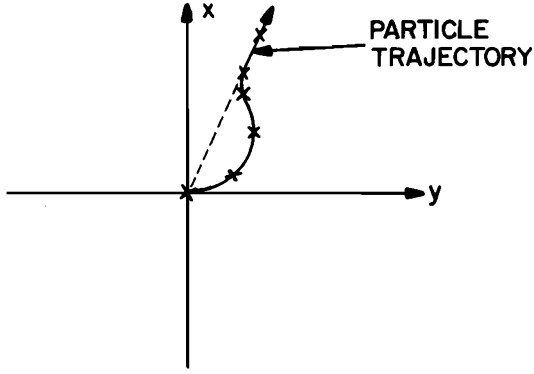

FIG. 1b

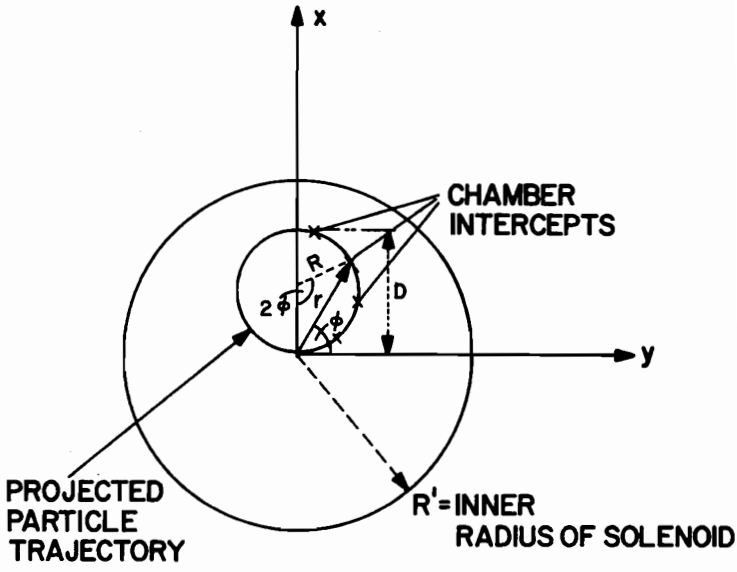
x
y
CHAMBER
INTERCEPTS
R
2φ
r
φ
D
PROJECTED
PARTICLE
TRAJECTORY
R'=INNER
RADIUS OF SOLENOID

FIG. 2

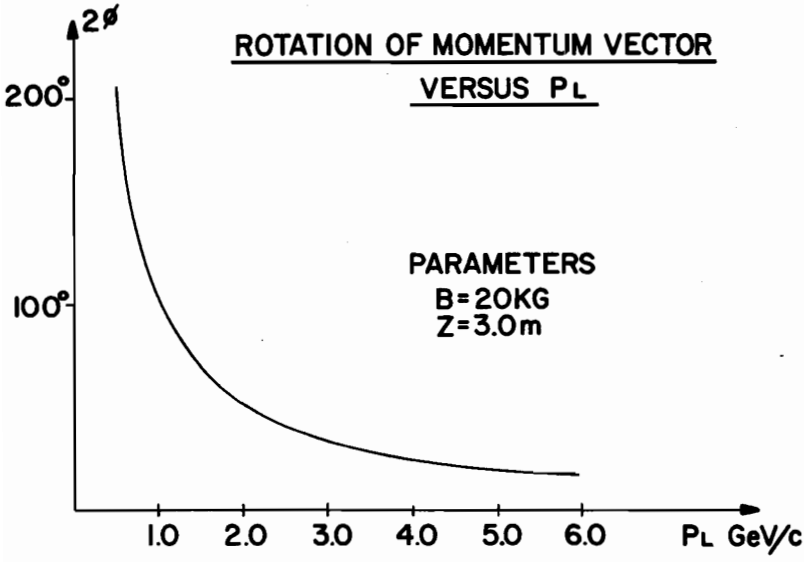
2ø
ROTATION OF MOMENTUM VECTOR
VERSUS PL
200°
100°
PARAMETERS
B=20KG
Z=3.0m
1.0
2.0
3.0
4.0
5.0
6.0
PL GeV/c

FIG. 3

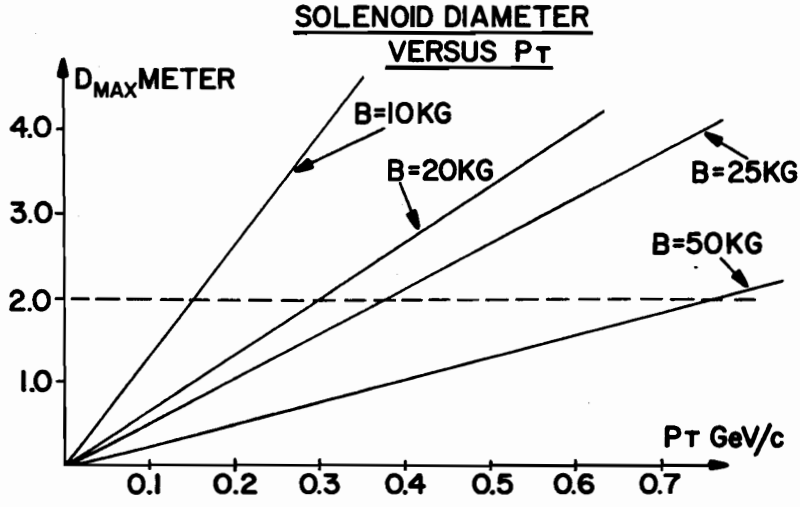
SOLENOID DIAMETER
VERSUS PT
DMAX METER
B=10KG
B=20KG
B=25KG
B=50KG
4.0
3.0
2.0
1.0
PT GeV/c
0.1
0.2
0.3
0.4
0.5
0.6
0.7

FIG.4

DIPOLE VERTEX SPECTROMETER

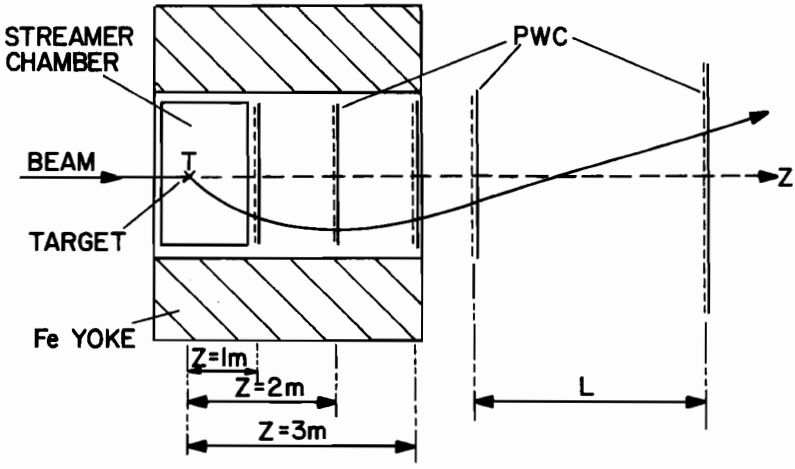

FIG. 5a

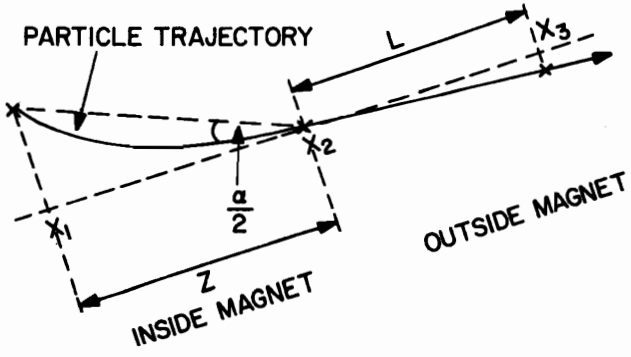

FIG. 5b

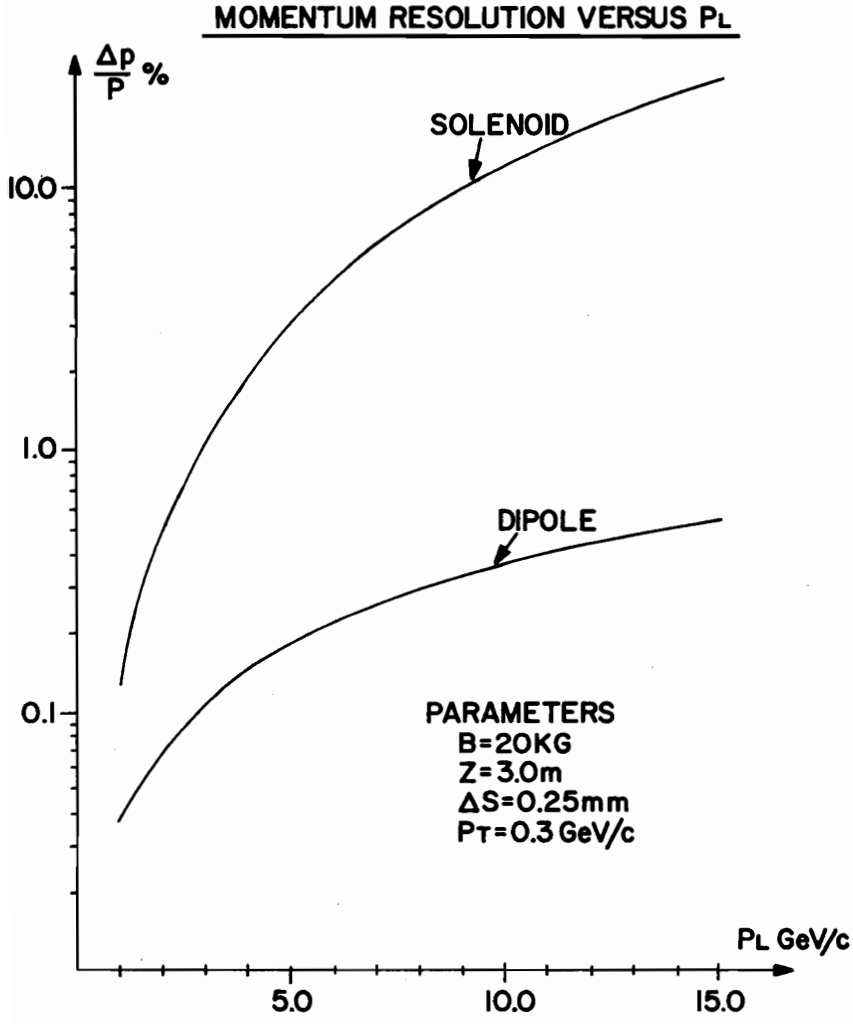
MOMENTUM RESOLUTION VERSUS PL
Δp/P %
SOLENOID
DIPOLE
10.0
1.0
0.1
PARAMETERS
B=20KG
Z=3.0m
ΔS=0.25mm
PT=0.3 GeV/c
PL GeV/c
5.0
10.0
15.0

FIG.6

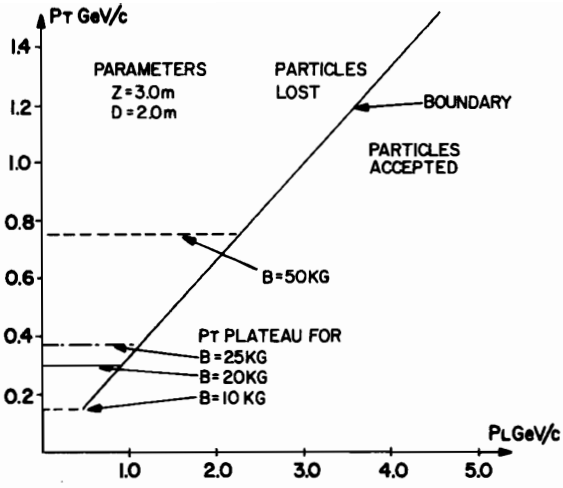

PT VERSUS PL ACCEPTANCE BOUNDARY FOR A SOLENOID

FIG.7

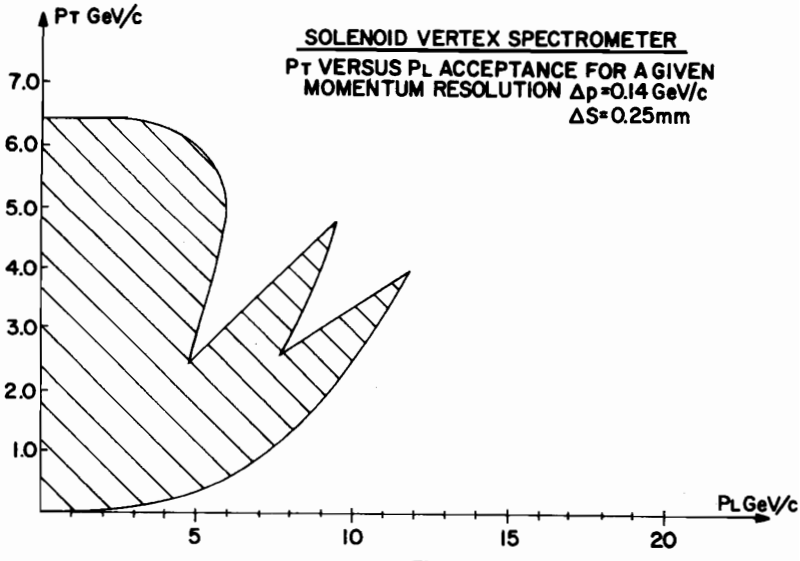

FIG.8

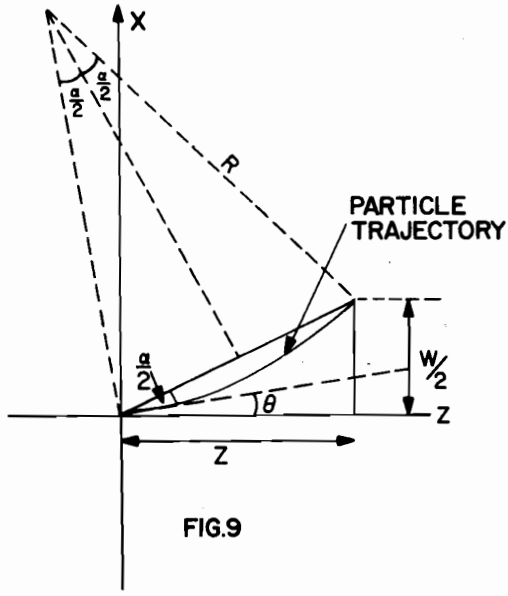
X
R
PARTICLE
TRAJECTORY
W/2
Z
θ
Z

FIG.9

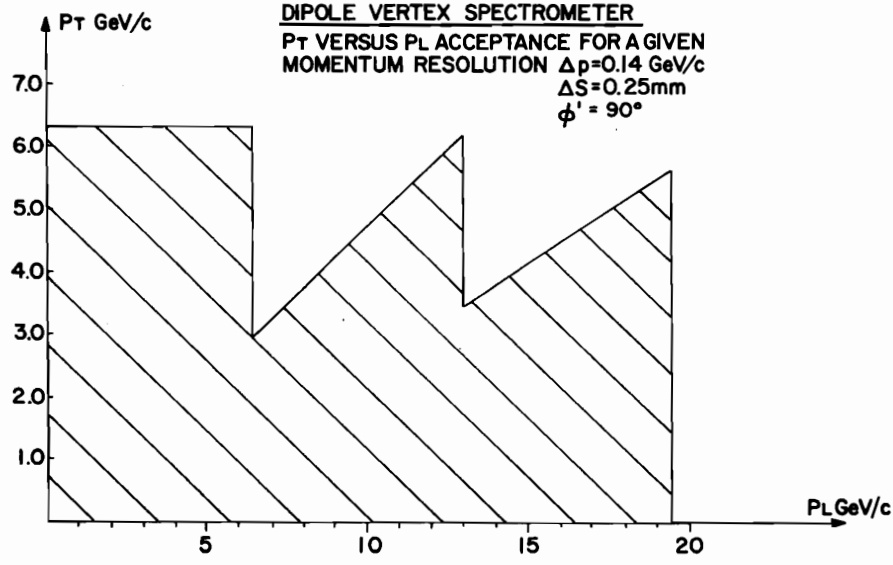
DIPOLE VERTEX SPECTROMETER
PT VERSUS PL ACCEPTANCE FOR A GIVEN
MOMENTUM RESOLUTION Δp=0.14 GeV/c
ΔS=0.25mm
φ' = 90°
PT GeV/c
7.0
6.0
5.0
4.0
3.0
2.0
1.0
5
10
15
20
PL GeV/c

FIG. 10

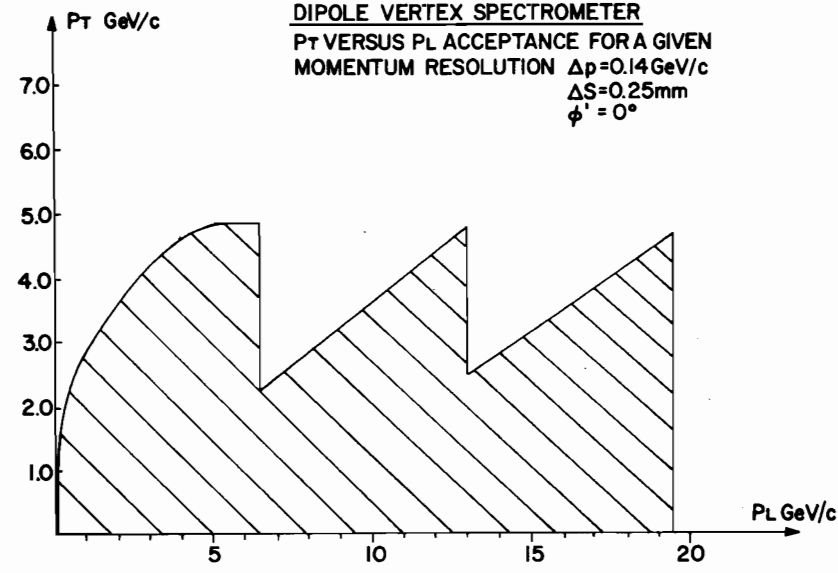
DIPOLE VERTEX SPECTROMETER
PT VERSUS PL ACCEPTANCE FOR A GIVEN
MOMENTUM RESOLUTION Δp=0.14GeV/c
ΔS=0.25mm
φ' = 0°
PT GeV/c
7.0
6.0
5.0
4.0
3.0
2.0
1.0
5
10
15
20
PL GeV/c

FIG.11

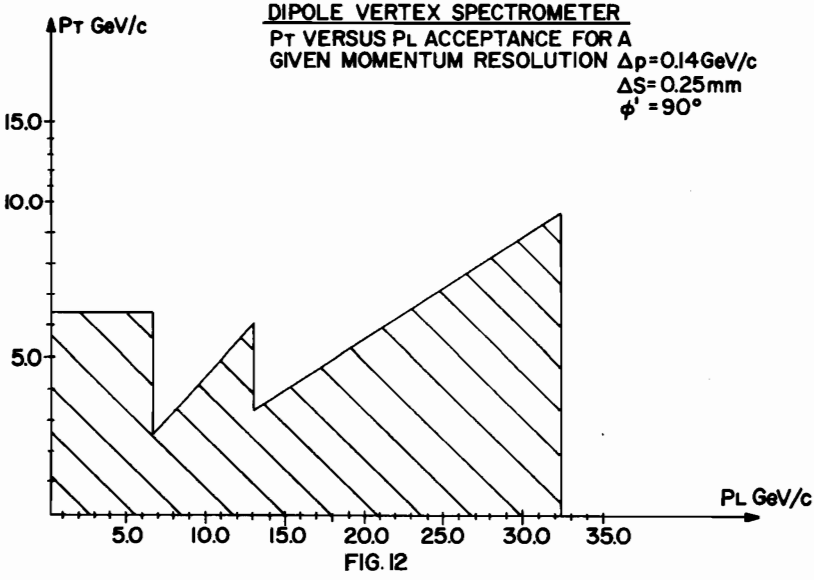
DIPOLE VERTEX SPECTROMETER
PT VERSUS PL ACCEPTANCE FOR A
GIVEN MOMENTUM RESOLUTION Δp=0.14GeV/c
ΔS= 0.25mm
φ' =90°
PT GeV/c
15.0
10.0
5.0
5.0
10.0
15.0
20.0
25.0
30.0
35.0
PL GeV/c

FIG. 12

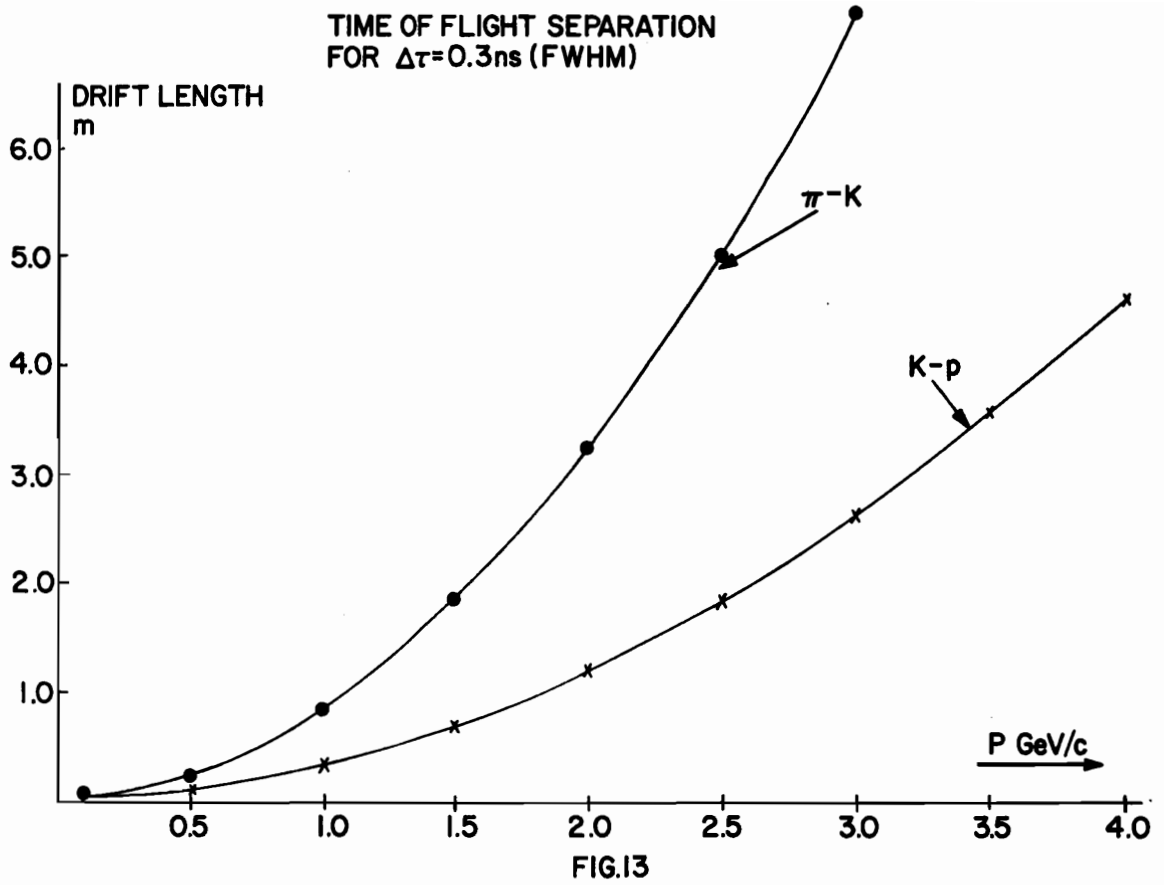
TIME OF FLIGHT SEPARATION
FOR Δτ=0.3ns (FWHM)
DRIFT LENGTH
m
6.0
5.0
4.0
3.0
2.0
1.0
π-K
K-p
P GeV/c
0.5
1.0
1.5
2.0
2.5
3.0
3.5
4.0

FIG.13